Lagrangian Velocity Distributions in a High-Resolution Numerical Simulation of the North Atlantic

ANNALISA BRACCO

The Abdus Salam International Centre for Theoretical Physics, Trieste, Italy

ERIC P. CHASSIGNET AND ZULEMA D. GARRAFFO

RSMAS/MPO, University of Miami, Miami, Florida

ANTONELLO PROVENZALE

Istituto di Cosmogeofisica del CNR, Turin, Italy

ABSTRACT

The statistical properties of Lagrangian velocities in a high-resolution numerical simulation of the North Atlantic Ocean are analyzed and discussed in the framework of particle dispersion parameterizations. Consistent with previous analyses of float trajectories, the modeled velocity distribution is shown to be non-Gaussian, both at the surface and at 1500 m. These results can have significant implications on oceanographic research, as they suggest that current parameterizations of particle dispersion by linear stochastic processes or eddy-diffusivity approaches may be incorrect, since they assume Gaussian velocity distributions. The results also indicate the need for empirical parameterizations of particle dispersion based on nonlinear stochastic processes. It is shown that, even for a truly non-Gaussian dataset, a Gaussian probability distribution function can be spuriously recovered when the sampling density is too low. The best compromise between data sampling and space averaging when a limited amount of data are available, as is the case in most field observations, is then identified.

1. Introduction

In the past 30 years, physical oceanographers have used Lagrangian data provided by neutrally buoyant floats to gain understanding of the ocean circulation (Rossby et al. 1975; Schmitz et al. 1981; Davis 1991; Bower and Lozier 1994; Richardson and Fratantoni 1999; Fratantoni 2001; Bower et al. 2002). Float data have also been used to characterize mesoscale turbulence in the ocean (Cheney et al. 1976; Bower and Rossby 1989; Richardson et al. 2000; LaCasce and Bower 2000), and their trajectories have been analyzed with the goal of developing statistical parameterizations of their dispersion (Davis 1987; Rupolo et al. 1996).

Since the introduction of a generalized advection–diffusion model to describe the effects of eddy variability on mean transport (Davis 1987, 1991), and, more recently, the application of stochastic particle models to turbulent dispersion in the ocean (Griffa et al. 1995;

Falco et al. 2000), the variance of the velocity fluctuations has been used to obtain estimates of turbulent diffusivities. The conditions under which these approaches are valid, however, require the turbulent velocity fluctuations to be Gaussian. In past years, several researchers have studied the velocity probability distribution functions (pdf's) provided both by subsurface floats and by surface drifters, with mixed results. Swenson and Niiler (1996) found Gaussian distributions for the zonal velocity component from surface drifters off California, along with non-normal statistics in the meridional direction. Bracco et al. (2000b) and Falco et al. (2000) found non-Gaussian distributions for subsurface floats deployed in the North Atlantic and for surface drifters in the Adriatic Sea, respectively. Conversely, Zhang et al. (2001) found that velocity distributions from RAFOS[1] floats launched in the Newfoundland basin were Gaussian in the limit of small bins. All of these field studies, however, failed to provide rigorous conclusions because of the low sampling density of floats

---

Corresponding author address: Prof. Eric P. Chassignet, RSMAS/MPO, University of Miami, 4600 Rickenbacker Causeway, Miami, FL 33149.
E-mail: echassignet@rsmas.miami.edu

[1] RAFOS (SOFAR spelled backwards) floats are similar to Sound Fixing and Ranging (SOFAR) floats, but with the moving floats receiving sound from a source in moored stations.

and drifters. Meanwhile, several studies of point–vortex systems and barotropic turbulence have shown that velocity pdf's in rotating turbulent flows are non-Gaussian at large enough Reynolds numbers (Min et al. 1996; Jiménez 1996; Weiss et al. 1998; Bracco et al. 2000a), because of the velocity field induced by the coherent vortices. That is, the non-Gaussian behavior of the velocity distribution is entirely due to the presence of coherent vortices. Compared to the idealized situations of point–vortex systems and barotropic turbulence, however, ocean mesoscale turbulence is much more complicated. It is not spatially homogeneous, and it is modulated by a large-scale circulation system.

In this paper, we study the velocity pdf's of particles seeded in a fine-mesh (grid spacing of 6 km on the average) numerical simulation of the North and equatorial Atlantic. Such a simulation exhibits a higher degree of complexity than barotropic turbulence and is not plagued by the lack of statistics and low sampling density that are typical of field studies. The analysis shows that, at midlatitudes, the one-particle velocity pdf's are non-Gaussian whenever a statistically significant number of data per bin are considered. This result holds for both surface drifters and subsurface floats. The departure from a normal distribution is confirmed for bins of $0.5° \times 0.5°$, that is, small enough to ensure resolution of the mean flow below the first Rossby deformation radius and complete separation of the mean velocity field from the turbulent (eddy) component. In the equatorial basin, however, nearly normal statistics are observed for the modeled subsurface floats. The difference between midlatitude and equatorial velocity statistics corroborates the results obtained by Bracco et al. (2000b) in the analysis of subsurface floats. Although limitations of the model include forcing with monthly climatology and errors introduced by numerical integration and interpolation, the results of this work support the view that mesoscale turbulence in the ocean is characterized by non-Gaussian velocity distributions.

Given the high density of the numerical floats/drifters, we are also able to perform a detailed investigation of the minimum number of data points needed in each bin in order to detect the real distribution and to avoid obtaining results that are dominated by a lack of statistics. Specifically, we show that, even for a truly non-Gaussian dataset, a Gaussian pdf is spuriously recovered when the sampling density in each bin is too low. We then identify the best compromise between data sampling and space averaging when a limited number of data are available, as is the case in most field observations.

The paper is organized as follows: sections 2 and 3 describe the numerical model and the simulated Lagrangian dataset, respectively. In section 4, we show the results of the analysis of the velocity distribution. A discussion of the results and some of the implications for the study of Lagrangian data are given in section 5.

2. The numerical model

A North Atlantic Ocean simulation has been carried out at very high resolution with the Miami Isopycnic Coordinate Ocean Model (MICOM) [see Bleck et al. (1992) and Bleck and Chassignet (1994) for a review of MICOM]. The computational domain is the Atlantic Ocean basin from 28°S to 65°N, including the Caribbean Sea and the Gulf of Mexico. The bottom topography is derived from a digital terrain dataset with 5′ latitude–longitude resolution (called ETOPO5). The surface boundary conditions are based on the Comprehensive Ocean–Atmosphere Data Set (COADS) monthly climatological data (da Silva et al. 1994). Open ocean boundaries are treated as closed but are outfitted with 3° buffer zones in which temperature and salinity are linearly relaxed toward their seasonally varying climatological values (Levitus 1982).

The horizontal grid is defined on a Mercator projection with resolution given by $1/12° \times 1/12° \cos\phi$, where ϕ is the latitude. The vertical density structure is represented by 15 isopycnic layers, topped by an active surface mixed layer. The vertical discretization was chosen to provide greater resolution in the upper part of the ocean. The model was spun up from rest for a total of 20 model years.

The high horizontal grid resolution (6 km on the average) drastically improved the model's behavior in comparison to that of previous coarse-resolution simulations. The major improvements are (i) a correct Gulf Stream separation and (ii) higher eddy activity. These results support the view that an inertial boundary layer, which results from the fine resolution, is an important factor in the separation process (Özgökmen et al. 1997), and that resolution of the first Rossby deformation radius is necessary for a correct representation of baroclinic instabilities. A more detailed description of this simulation, as well as a discussion of its strengths and weaknesses, can be found in Paiva et al. (1999), Garraffo et al. (2001a,b), and Chassignet and Garraffo (2001). Specifically, the analysis of sea surface height variability spectra performed by Paiva et al. (1999) found length scales representative of the simulated eddy field to be in good agreement with observations based on altimeter data.

3. The Lagrangian dataset

At the beginning of year 14 of the Eulerian simulation, a total of 10 000 isobaric Lagrangian particles are deployed at the surface and at depths of 1500 m on a regular $1° \times 1°$ grid (5000 particles at each level). The particle trajectories are numerically tracked for a period of 5 model years, and their positions (and derived velocities) are recorded every 12 h. Lagrangian particles are constrained to remain on an isobaric surface, and the trajectories are integrated by using the velocity projection on the isobaric surface where the particles reside.

Surface trajectories are calculated using the Eulerian surface velocity field that is representative of the depth-averaged mixed layer, which varies both seasonally and with latitude. The mixed layer depth is generally between 20 and 100 m, but occasionally it can reach 2000 m in high-latitude regions during deep water formation events (Smith et al. 2000).

The particles are numerically advected using a second-order Runge–Kutta scheme, with 16-point space interpolation in the ocean interior and 4-point near the coast. The advection time step is 2 h. In the integration of particle trajectories, the interpolation procedure can lead to deviations of a numerical trajectory from that of a fluid particle (Zouari and Babiano 1990). Even in a frozen time-independent divergence-free field, numerically integrated particles may not necessarily follow streamlines, because of interpolation effects: this is the case, for example, if one uses linear interpolation. Evaluation of our 16-point space interpolator with a known, frozen velocity field shows that the errors on individual trajectories due to interpolation are negligible for timescales up to at least 100 days. On longer timescales, the individual particle trajectories start to deviate from the trajectories of fluid particles released at the same initial position. That is, individual particles follow "good" fluid particle trajectories but slowly diffuse from one fluid parcel trajectory to another and do not trace the same fluid parcel for the whole integration period of 5 model years. However, the ensemble of trajectories still provides a reliable representation of the statistical properties of the velocity field. In the following analysis, individual trajectories do not spend more than 100 days in each individual bin, and thus they can be taken as representative of single fluid particle trajectories during the crossing of each bin.

A comparison between the surface trajectories and in situ drifter data has been performed by Garraffo et al. (2001b). The analysis of eddy kinetic energy and root-mean-square velocity indicates that the numerical model is able to reproduce the location of the maxima and minima of the eddy root-mean-square velocity, but it underestimates the eddy kinetic energy in the Gulf Stream extension and in the ocean interior. Additionally, in the interior, the Lagrangian timescale for the simulated trajectories is longer by approximately a factor of 2 than for the in situ drifters. This is likely due primarily to the lack of high-frequency winds in the model forcing and to the fact that there is no vertical shear in the bulk mixed layer (Garraffo et al. 2001b). Mean flow estimates, on the other hand, show a good overall agreement between the numerical trajectories and the observations (Garraffo et al. 2001a,b).

In this paper, we focus on the 10 000 particles seeded in the mixed layer and at 1500 m. The total number of positions for the 5-yr period is about 9 000 000 for each set. The surface data were chosen because of the existing detailed comparison between the modeled and in situ trajectories performed by Garraffo et al. (2001b). The particles deployed at 1500 m allow us to compare the velocity distributions of our modeled trajectories with the analysis performed by Bracco et al. (2000b) on "deep floats" in the North Atlantic. In that work, the deep dataset grouped together all available trajectories below 1000-m depth, but the most significant portion of the data (about 65% of the total) was from deployments between 1000 and 2000 m.

4. Velocity distributions

In this section, we discuss the results of the analysis of the two sets of model Lagrangian data described above. The numerical model provides the zonal and meridional positions of the floats as a function of time, $X(t)$ and $Y(t)$, and the corresponding Lagrangian velocity components, $U(t)$ and $V(t)$.

In the analysis of the statistical properties of ocean mesoscale turbulence, it is important to distinguish between "geographical" variations of the average quantities, related to the presence of large-scale dynamics such as the gyre system, and "turbulent" inhomogeneities, due to the intrinsic dynamics of mesoscale turbulence and mesoscale eddies. Usually, this separation is achieved by defining an ensemble of spatiotemporal bins over which the data are averaged. The average quantities define the large-scale flows, while the statistical properties inside the bins allow for estimating the properties of mesoscale turbulence (see, e.g., Owens 1991). Clearly, the whole procedure resides on the definition of the bin size that separates large-scale motions from mesoscale dynamics. The choice of the critical bin size is somewhat arbitrary, and the concept of a unique bin size that separates two regimes can be questioned. In addition, a well-defined scale separation between large-scale flows and mesoscale turbulence should be present in order for such a binning procedure to be effective. Although the binning procedure remains a heuristic approach, Stammer (1997) showed that when bin sizes of 0.5° or smaller are used, the first Rossby deformation radius is resolved over the whole domain, thereby raising the possibility of filtering out the large-scale components.

In the following analysis, we adopt a binning procedure and consider how the results depend on the bin size. The mean velocity components, $\langle U \rangle$ and $\langle V \rangle$, and the rms deviations from the mean for the two datasets, are estimated as area–time averages computed over different bin sizes, from 0.25° × 0.25° to 3° × 3°, and over the 5-yr period. Although the initial sampling is uniform because the floats are deployed on a regular 1° × 1° grid, the data distribution is nonuniform, especially for the surface trajectories. A higher sampling density is found in the subtropical convergence zone, while the equatorial divergence zone is undersampled by the numerical tracers because of wind-driven Ekman transport, as noted by Garraffo et al. (2001b). Large gradients in the sampling density can introduce a bias in the eval-
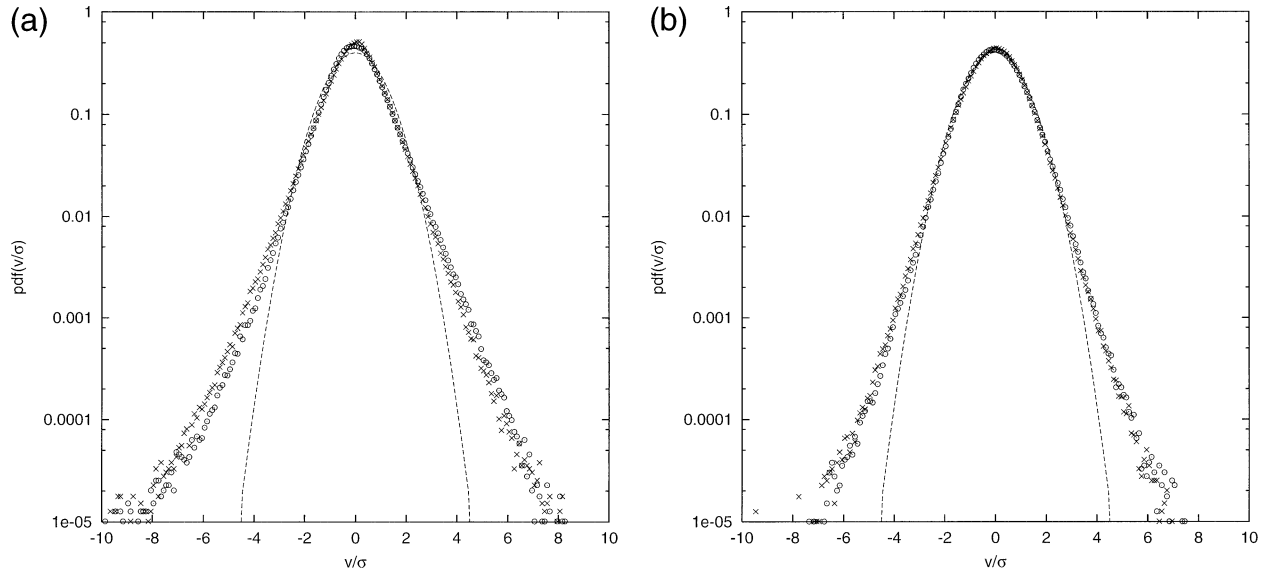
FIG. 1. Velocity distributions for numerically simulated (a) surface drifters and (b) 1500-m floats in the North Atlantic. The data have been normalized into 0.5° × 0.5° bins as discussed in the text. The zonal (×) and meridional (○) components of the eddy velocity field are shown separately. The dashed line shows a Gaussian distribution with the same variance.

uation of the mean flow circulation. To ensure statistical reliability, bins with less than 100 events are discarded. This point is further discussed below.

Inside each bin, the differences between individual values of the Lagrangian velocity components and the local space–time means, $u = U - \langle U \rangle$ and $v = V - \langle V \rangle$, are assumed to represent the eddy (turbulent) velocity components. The distribution of eddy velocities inside each bin is normalized to unit variance, and the average pdf of eddy velocities is then obtained as an average over the pdf's obtained for the individual bins. The procedure of removing the mean and normalizing to unit variance the pdf inside each bin assures removal of geographical inhomogeneities at scales larger than the bin size, while inhomogeneities at scales smaller than the bin size are preserved.

Figures 1a and 1b show the average velocity pdf's in the North Atlantic (north of 15°N) for floats at the surface and at 1500 m, respectively. The bin size is 0.5° × 0.5°. The distributions are clearly non-Gaussian, with extended high-velocity tails. The kurtoses of the average velocity distributions, $k = \langle u^4 \rangle / \langle u^2 \rangle^2$, vary from a minimum of 3.69 for the meridional component of deep trajectories to a maximum of 4.86 for the zonal component in the surface mixed layer (the kurtosis of a normal distribution has a value of $k = 3$). Due to the extremely high number of realizations in each dataset (about 6 000 000 velocities are concentrated north of 15°N), common statistical tools, such as the Kolmogorov–Smirnov or χ^2 tests, indicate rejection of the null hypothesis of a Gaussian distribution at a confidence level higher than 99.9%. Note that in this study we prefer to analyze zonal and meridional velocities sep-

arately, because of the anisotropy of the system induced by differential rotation. At small enough bin size, isotropy should return and the two distributions should converge to each other, as has been effectively observed.

Maps of the kurtoses of zonal velocities in the North and equatorial Atlantic are shown in Figs. 2a and 2b for floats at the surface and at 1500 m, respectively, calculated on individual bins of size 0.5°. As anticipated, the southern boundary of the subtropical gyre and the equatorial upwelling region are poorly sampled by surface drifters and thus are excluded from the present analysis. These figures indicate that the Lagrangian velocities obtained from the model at midlatitudes are non-Gaussian both below the thermocline and in the surface mixed layer. By contrast, model Lagrangian velocities at 1500 m in the equatorial Atlantic are normally distributed, with the exception of the boundary region immediately south of the equator, in agreement with previous analysis of field data (Bracco et al. 2000b). The kurtoses of meridional velocities (not shown) are substantially similar, except for a small region of Gaussianity in the Gulf Stream extension for the model surface dataset. In the Gulf Stream, model meridional velocities are extremely small and the signal is dominated by noise. These small meridional velocities are a well-known signature of a jet, which acts as a transport barrier in the meridional direction (Pratt et al. 1995; Rogerson et al. 1999; Berloff et al. 2002).

5. Effects of bin size and sampling density

As mentioned in the previous section, an important variable in the analysis is the choice of the bin size. A
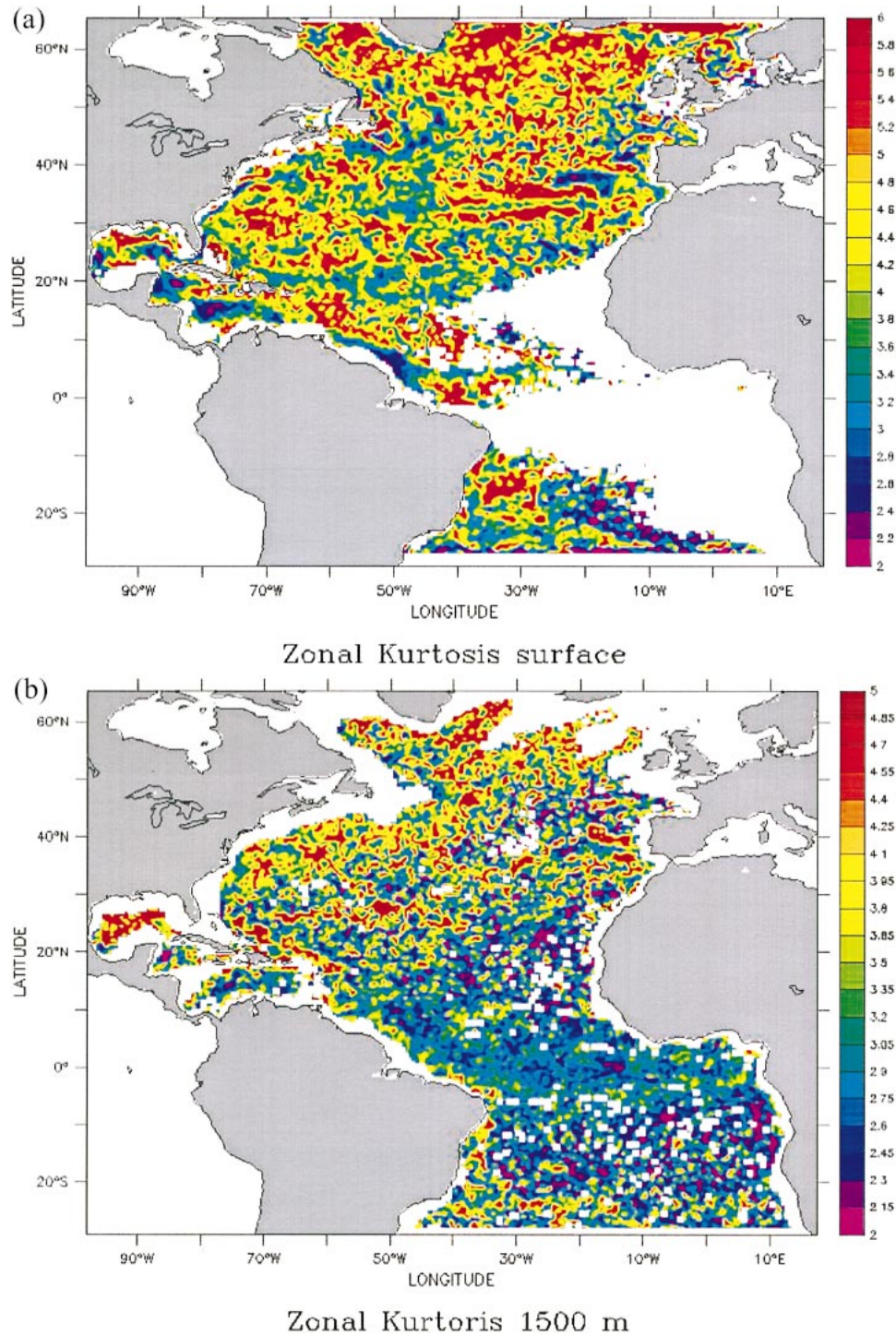
FIG. 2. Maps of the zonal kurtosis of the turbulent velocity components from model Lagrangian tracers at (a) the surface and (b) 1500 m. The data have been normalized into $0.5° \times 0.5°$ bins.

bin size that is too large may lead to the inclusion of larger-scale geographical inhomogeneities and therefore affect the value of the kurtosis. This is illustrated by Fig. 3, which shows the variation of the kurtosis of the velocity distributions as the bin size is varied from 0.25°

to 3°: there is a trend toward smaller values of the kurtosis as the size of the bins decreases. Below bin sizes of 0.5°, the kurtosis does not change significantly and differences are contained within the error bars, suggesting that the statistics are no longer influenced by
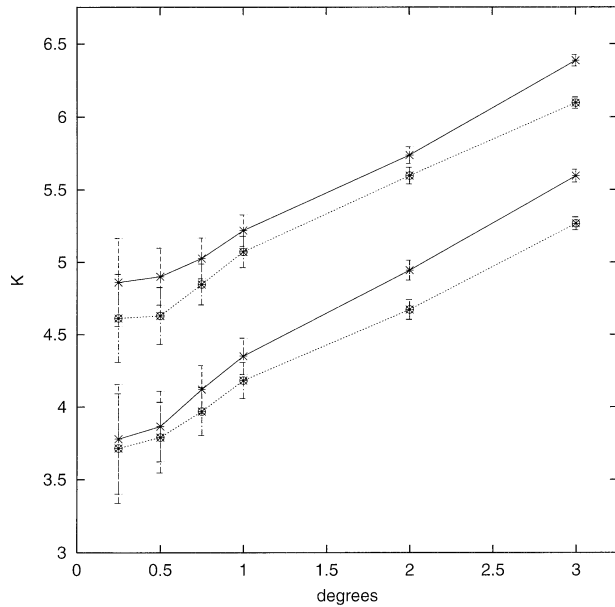
FIG. 3. Variation of the kurtosis of the velocity distributions from model Lagrangian trajectories at the surface (*) and at 1500 m ($\otimes$) as a function of the bin size. The two components, zonal (full line) and meridional (dotted line), are shown separately.

inhomogeneities of the mean flow (as already stated in the previous section). However, with the smallest bin sizes the sampling density becomes rather poor, and the statistical results are less reliable because there are fewer degrees of freedom in each box.

Error bars for the values of the kurtosis are provided in Fig. 3. This raises the issue of how best to evaluate the uncertainty and the significance of statistical results. When velocity pdf's are calculated from in situ observations, the two most important types of errors are measurement errors and sampling effects. In numerical simulations, measurement errors are replaced by model roundoff, interpolation errors, and model uncertainties [see Garraffo et al. (2001b) and Chassignet and Garraffo (2001) for a discussion of the model results]. Sampling effects, on the other hand, are present both in field data and in numerically simulated trajectories, since they are related to the amount of available data. As will be shown in the remainder of this section, sampling errors can sometimes lead to spurious results.

In order to quantify sampling errors, we make the assumption that the measurements are drawn from a stationary and quasi-normal process.[2] The rms error for each mean velocity component in a specified bin (Flierl

___

[2] By quasi-normal here, we mean a process with finite variance. The physical processes involved in the dynamics of the oceans are neither stationary nor necessarily quasi-normal. This assumption has the advantage of greatly simplifying the evaluation of the error on each measurement, and it does not significantly affect our conclusions.
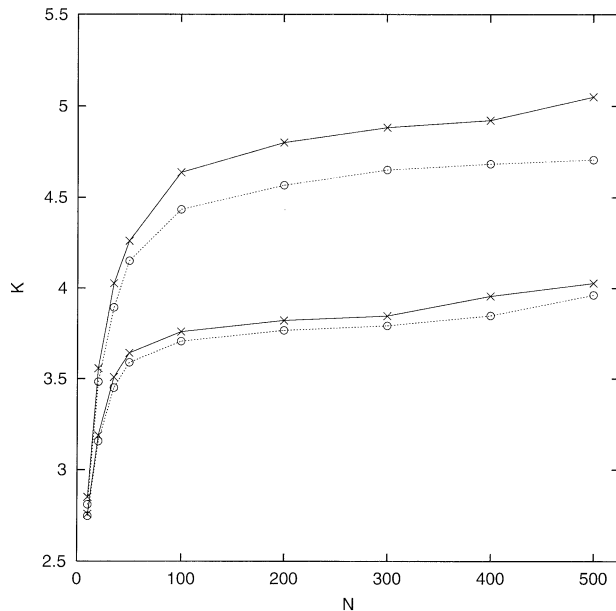
and McWilliams 1977; Riser and Rossby 1983; Owens 1991; Davis 1991) is then given by

$$\varepsilon(u) = (\sigma^2/N^*)^{1/2}, \qquad (1)$$

where σ^2 is the velocity variance and N^* is the number of independent events in the bin. In the case of single trajectories, N^* can be approximated by

$$N^* \approx N\Delta t/2T, \qquad (2)$$

where N is the total number of measurements in the bin, Δt is the sampling interval, and T is the Lagrangian integral timescale.

For different bins, the mean and the variance will have different values. The distribution of the means and variances obtained from these bins is then characterized by a variance that depends on the number of independent observations in each bin. The distribution becomes narrower as the number of observations in each bin gets larger. In general, for processes with finite variance, the distribution of the means is Gaussian, because of the central limit theorem.

When we compute the average pdf, normalizing the data in each bin to the local mean and variance, we convolve the original distribution of the data under study with that of the local means. If the latter distribution is "broad" (i.e., if it has a large variance due to the fact that we have too few data in each bin), then it dominates the statistics and masks the original distribution of the data. In this case, we can say that the results are entirely dominated by sampling errors. The minimum number of points required to resolve a given distribution depends on the shape of the distribution under study, and it results from a trade-off between the non-Gaussianity of the original pdf and the Gaussian behavior induced by poor sampling. This minimum number of points can be determined by requiring the kurtosis of the observed distribution to be significantly different (at a prescribed level) from the Gaussian value.

To quantify this effect for the case of float trajectories, we show in Fig. 4 the kurtosis for a fixed bin size ($0.5°$ $\times$ $0.5°$), as a function of the number of (independent) data points in each box. The measurements in each box were selected by discarding multiple realizations from the same particle trajectory, unless otherwise constrained by the limited sampling. When bins with less than about 30 events are used, the results are strongly biased by the sampling error. In this case, the insufficient sampling induces an artificial drop in the kurtosis, which then takes values close to 3, erroneously suggesting that the distribution is Gaussian. Below about 30 independent observations per box, the null hypothesis of Gaussian velocity distributions cannot be rejected. We also note that the anisotropy between the zonal and meridional velocity components, originally present in the properly sampled data, is lost as the number of measurements in each bin decreases. On the other hand, there are only small variations in the values of the kurtosis and in the shape of the distribution when the num-

FIG. 4. Variation of the kurtosis of the model velocity distributions normalized in $0.5° \times 0.5°$ boxes for tracers at the surface ($\times$) and at 1500 m ($\bigcirc$) as a function of the number of measurements per box, N. The two components, zonal (full line) and meridional (dotted line), are shown separately.

ber of observations increases from 100 to 400. An analysis was performed with analogous results for a synthetic distribution with Gaussian core and exponential tails (Pasquero et al. 2001), with results similar to those observed for the velocity field of barotropic turbulence.

In summary, whenever less than a minimum of 30 observations per $0.5° \times 0.5°$ bin are considered, the estimated Lagrangian velocity distributions do not provide information on any physical process, since they are totally dominated by the (Gaussian) distribution of sampling errors.

6. Discussion and conclusions

The analysis of Lagrangian velocity distributions in a fine mesh numerical simulation of the North Atlantic indicates that Lagrangian velocities are non-Gaussian in oceanic regions characterized by high mesoscale activity, in agreement with the results discussed by Bracco et al. (2000b) for ocean float trajectories. The high Lagrangian sampling density achieved by the numerical model allows us to remove the mean flow signature at scales smaller than the first baroclinic Rossby deformation radius. This leads to the interpretation that non-Gaussianity is generated by intrinsic dynamical inhomogeneities of mesoscale turbulence and not by larger-scale "geographical" inhomogeneities of the mean flow.

The practice commonly used to remove large-scale flows from Lagrangian data, which is adopted here, is

to bin the data into small boxes, compute the pdf in each box, and then average the normalized pdf's. In the analysis of float data, however, an important limitation arises due to the sparse statistics that have been available up to now. Often, the sampling density inside each bin is too limited to allow for a reliable statistical characterization of the local properties of mesoscale turbulence. Nor can the bin size be increased at will, because of the danger in mixing local turbulence and large-scale dynamics. Thus, a compromise is usually made between the bin size, which must be small enough to resolve and remove the effects of large-scale inhomogeneities, and the number of available observations for each bin, which must be large enough to ensure statistical significance of the results. These two requirements may be too stringent, and failure to satisfy them can lead to the detection of false non-Gaussianity if the bins are too large, or of spurious Gaussianity if the statistics inside each bin are too poor.

The results of the present work show that the binning approach to the study of Lagrangian velocity statistics in the ocean is meaningful only if a minimum of about 30 independent data points per $0.5° \times 0.5°$ box are available. Below this approximate threshold, isotropy and Gaussianity in the data distributions cannot be considered as a physical signature, as they simply reflect the distribution of sampling errors. Low sampling density may be one of the reasons for the disagreement between the recent results of Zhang et al. (2001), who found isotropic and Gaussian Lagrangian statistics in the North Atlantic Current region, and those of previous works (Poulain et al. 1996; Krauss and Böning 1987; Sundermeyer and Price 1998; Bracco et al. 2000b).

Finally, we must comment on the physical origin of the non-Gaussian velocity pdf's. In past studies of quasi-geostrophic turbulence, non-Gaussian velocity pdf's were shown to be generated by the presence of coherent vortices (Min et al. 1996; Jiménez 1996; Weiss et al. 1998; Bracco et al. 2000a). Even though long-lived coherent vortices do permeate the ocean, real geophysical flows are much more complicated than homogeneous quasi-geostrophic turbulence. Vortices are not the only coherent structures that must be taken into account. Jets and waves induce further signatures on the motion of Lagrangian tracers. As pointed out by Falco et al. (2000), the eddy velocity component includes "actual eddies due to instabilities as well as wave phenomena, wind-driven current reversals, and possible long-term variability at seasonal and interannual scales." D'Asaro and Lien (2000) recently used Lagrangian frequency spectra from float trajectories to distinguish internal gravity waves and turbulence. They concluded that the division between waves and turbulence is not sharp in the data. Theoretical models and high-resolution numerical simulations such as the one discussed in this paper can provide useful tools to better identify and understand the dynamical influence

of the different processes involved in ocean turbulence. These topics are the focus of a separate study, now in progress.

REFERENCES

Berloff, S. P., J. C. McWilliams, and A. Bracco, 2002: Material transport in oceanic gyres. Part I: Phenomenology. *J. Phys. Oceanogr.,* **32,** 764–796.

Bleck, R., and E. P. Chassignet, 1994: Simulating the oceanic circulation with isopycnic-coordinate models. *The Oceans: Physical-Chemical Dynamics and Human Impact,* S. K. Majundar, Ed., The Pennsylvania Academy of Science, 17–39.

——, C. Rooth, D. Hu, and L. T. Smith, 1992: Salinity-driven thermocline transients in a wind- and thermohaline-forced isopycnic coordinate model of the North Atlantic. *J. Phys. Oceanogr.,* **22,** 1486–1505.

Bower, A. S., and H. T. Rossby, 1989: Evidence of cross-frontal exchange processes in the Gulf Stream based on isopycnal RAFOS float data. *J. Phys. Oceanogr.,* **19,** 1177–1190.

——, and M. S. Lozier, 1994: A closer look at particle exchange in the Gulf Stream. *J. Phys. Oceanogr.,* **24,** 1399–1418.

——, and Coauthors, 2002: Directly measured mid-depth circulation in the northeastern North Atlantic Ocean. *Nature,* **419,** 603–607.

Bracco, A., J. LaCasce, C. Pasquero, and A. Provenzale, 2000a: The velocity distribution of barotropic turbulence. *Phys. Fluids,* **12,** 2478–2488.

——, ——, and A. Provenzale, 2000b: Velocity probability density functions for oceanic floats. *J. Phys. Oceanogr.,* **30,** 461–474.

Chassignet, E. P., and Z. D. Garraffo, 2001: Viscosity parameterization and the Gulf Stream separation. *From Stirring to Mixing in a Stratified Ocean: Proc. 'Aha Huliko'a Hawaiian Winter Workshop,* Honolulu, HI, University of Hawaii at Manoa, 37–41.

Cheney, R. E., W. H. Gemmill, M. K. Shank, P. L. Richardson, and D. C. Webb, 1976: Tracking a Gulf Stream ring with SOFAR floats. *J. Phys. Oceanogr.,* **6,** 741–749.

D'Asaro, E. A., and R.-C. Lien, 2000: Lagrangian measurements of waves and turbulence in stratified flows. *J. Phys. Oceanogr.,* **30,** 641–655.

da Silva, A. M., C. C. Young, and S. Levitus, 1994: *Algorithms and Procedures.* Vol. 1, *Atlas of Surface Marine Data,* NOAA Atlas NESDIS 6, 83 pp.

Davis, R. E., 1987: Modeling eddy transport of passive tracers. *J. Mar. Res.,* **45,** 635–666.

——, 1991: Observing the general circulation with floats. *Deep-Sea Res.,* **38,** 531–571.

Falco, P., A. Griffa, P.-M. Poulin, and E. Zambianchi, 2000: Transport properties in the Adriatic Sea as deduced from drifter data. *J. Phys. Oceanogr.,* **30,** 2055–2071.

Flierl, G. R., and J. C. McWilliams, 1977: On the sampling requirements for measuring moments of eddy variability. *J. Mar. Res.,* **35,** 797–820.

Fratantoni, D. M., 2001: North Atlantic surface circulation during the 1990's observed with satellite-tracked drifters. *J. Geophys. Res.,* **106,** 22 067–22 093.

Garraffo, Z. D., A. Griffa, A. J. Mariano, and E. P. Chassignet, 2001a: Lagrangian data in a high-resolution numerical simulation of the North Atlantic. II. On the pseudo-Eulerian averaging of Lagrangian data. *J. Mar. Syst.,* **29,** 177–200.

——, A. J. Mariano, A. Griffa, C. Veneziani, and E. P. Chassignet, 2001b: Lagrangian data in a high-resolution numerical simulation of the North Atlantic. I. Comparison with in situ drifter data. *J. Mar. Syst.,* **29,** 157–176.

Griffa, A., K. Owens, L. Piterbarg, and B. Rozovskii, 1995: Estimates of turbulence parameters from Lagrangian data using a stochastic particle model. *J. Mar. Res.,* **53,** 371–401.

Jiménez, J., 1996: Probability density in two-dimensional turbulence. *J. Fluid Mech.,* **313,** 223–240.

Krauss, W., and C. W. Böning, 1987: Lagrangian properties of eddy fields in the northern North Atlantic as deduced from satellite-tracked buoys. *J. Mar. Res.,* **45,** 259–291.

LaCasce, J. H., and A. S. Bower, 2000: Relative dispersion in the subsurface North Atlantic. *J. Mar. Res.,* **58,** 863–894.

Levitus, S., 1982: *Climatological Atlas of the World Ocean.* NOAA Prof. Paper 13, 173 pp. and 17 microfiche.

Min, I. A., I. Mézic, and A. Leonard, 1996: Levy stable distributions for velocity and velocity difference in system of vortex elements. *Phys. Fluids,* **8,** 1169–1180.

Owens, W. B., 1991: A statistical description of the mean circulation and eddy variability in the northwestern North Atlantic using SOFAR floats. *Progess in Oceanography,* Vol. 28, Pergamon, 257–303.

Özgökmen, T. M., E. P. Chassignet, and A. Paiva, 1997: Impact of wind forcing, bottom topography, and inertia on mid-latitude jet separation in a quasigeostrophic model. *J. Phys. Oceanogr.,* **27,** 2460–2476.

Paiva, A., J. Hargrove, E. Chassignet, and R. Bleck, 1999: Turbulent behavior of the fine-mesh (1/12 degree) numerical simulation of the North Atlantic. *J. Mar. Syst.,* **21,** 307–320.

Pasquero, C., A. Provenzale, and A. Babiano, 2001: Parameterization of dispersion in two-dimensional turbulence. *J. Fluid Mech.,* **439,** 279–303.

Poulain, P.-M., A. Warn-Varnas, and P. P. Niiler, 1996: Near-surface circulation of the Nordic seas as measured by Lagrangian drifters. *J. Geophys. Res.,* **101,** 18 237–18 258.

Pratt, L., S. Lozier, and N. Belyakova, 1995: Parcel trajectories in quasigeostrophic jets: Neutral modes. *J. Phys. Oceanogr.,* **25,** 1451–1466.

Richardson, P. L., and D. M. Fratantoni, 1999: Float trajectories in the Deep Western Boundary Current and deep equatorial jets of the tropical Atlantic. *Deep-Sea Res.,* **46,** 305–333.

——, A. S. Bower, and W. Zenk, 2000: A census of Meddies tracked by floats. *Progress in Oceanography,* Vol. 45, Pergamon, 209–250.

Riser, S. C., and H. T. Rossby, 1983: Quasi-Lagrangian structure and variability of the subtropical western North Atlantic circulation. *J. Mar. Res.,* **41,** 127–162.

Rogerson, A., P. Miller, L. Pratt, and C. Jones, 1999: Lagrangian motion and fluid exchange in a barotropic meandering jet. *J. Phys. Oceanogr.,* **29,** 2635–2655.

Rossby, T., A. D. Voorhis, and D. C. Webb, 1975: A quasi-Lagrangian study of mid-ocean variability using long range SOFAR floats. *J. Mar. Res.,* **33,** 335–382.

Rupolo, V., B.-L. Hua, A. Provenzale, and V. Artale, 1996: Lagrangian spectra at 700 m in the western North Atlantic. *J. Phys. Oceanogr.,* **26,** 1591–1607.

Schmitz, W. J., Jr., J. F. Price, P. L. Richardson, W. B. Owens, D. C. Webb, R. E. Cheney, and H. T. Rossby, 1981: A preliminary exploration of the Gulf Stream system with SOFAR floats. *J. Phys. Oceanogr.,* **11,** 1194–1204.

Smith, L. T., E. P. Chassignet, and R. Bleck, 2000: The impact of lateral boundary conditions and horizontal resolution on North Atlantic water mass transformation and pathways in an isopycnic coordinate ocean model. *J. Phys. Oceanogr.,* **30,** 137–159.

Stammer, D., 1997: Global characteristics of ocean variability estimated from regional TOPEX/POSEIDON altimeter measurements. *J. Phys. Oceanogr.,* **27,** 1743–1769.

Sundermeyer, M. A., and J. F. Price, 1998: Lateral mixing and the North Atlantic tracer release experiment: Observations and numerical simulations of Lagrangian particles and a passive tracer. *J. Geophys. Res.,* **103,** 21 481–21 497.

Swenson, M. S., and P. P. Niiler, 1996: Statistical analysis of the surface circulation of the California Current. *J. Geophys. Res.,* **101,** 22 631–22 645.

Weiss, J. B., A. Provenzale, and J. C. McWilliams, 1998: Lagrangian dynamics in high-dimensional point-vortex systems. *Phys. Fluids,* **10,** 1929–1941.

Zhang, H.-M., M. D. Prater, and T. Rossby, 2001: Isopycnal Lagrangian statistics from the North Atlantic Current RAFOS float observations. *J. Geophys. Res.,* **106,** 13 817–13 836.

Zouari, N., and A. Babiano, 1990: Experiences numeriques Lagrangiennes a partir de modeles Euleriens. *Atmos.–Ocean,* **28,** 345–357.